Online computational tools dedicated to the detection of induction machine faults

Abdesselam Lebaroud *, Ammar Medoued

Université 20 Août 1955 et Laboratoire LGEC, B.P. 26 route d'El-Hadaiek, Skikda-21000, Algeria

ARTICLE INFO

ABSTRACT

This paper presents online components calculation techniques for stator and rotor of the induction machine. Four techniques have been developed for online components calculation; the first one starts the calculation of the negative component of stator current space vector using the Discrete Fourier Transform (DFT) in order to detect the stator fault. The second technique is dealing with the detection of rotor fault by the Recursive Fourier Transform (RFT), This technique improves the signal acquisition and enhanced detection of components near the fundamental. The third technique allows improving of the rotor fault detection by the spectrum of analytical signal. The fourth and the last technique is the frequency analysis of the instantaneous power, which allows obtaining a singular signature of faults. These techniques have shown better detection, where each fault is characterized by a singular signature and therefore they improve the detection and diagnosis of faults. Experimental results applied on an asynchronous machine 5.5 kW, approve and validate these calculation techniques.

© 2012 Elsevier Ltd. All rights reserved.

1. Introduction

A variety of faults can occur within induction motors, during normal operation. Several faults, such as unbalanced stator, broken rotor bars, rotor eccentricity, can result in a complete breakdown of the machine, if the progress of the fault is not detected. The machine parameters which are most often monitored include line current, leakage flux, and vibration. Line current is probably the most convenient of these parameters, since in an industrial environment it is the most accessible parameter, this can be measured remotely if needed, and requires simple instrumentation. In recent years many research works have been carried out on the monitoring condition and diagnosis of electrical machines. Many tools of calculation have been proposed for electrical machine faults detection and localization. These tools include the measurement of stator current and voltage, torque, external magnetic flux density and vibration. On-line calculation of induction machine faults such as broken rotor bars and stator unbalanced can be carried out by analyzing the stator current by temporal or spectral, or both at once as time–frequency. Broken rotor bars result in twice slip frequency sidebands around the fundamental frequency of stator current, while unbalanced stator, such as stator winding short circuits, which cause changes in three-phase stator current system and the occurrence of negative sequence current. Many diagnostic techniques for induction motors have been reported in the literature as to diagnose electric machine faults, Therefore some researchers have investigated the monitoring of machine conditions, mainly based

on the signature of external variables, for instance by means of all voltage and current signals, speed, torque and instantaneous power. They can be computed, and more information may be retrieved for diagnostic purpose. The Park's vector approach and the motor angular fluctuation of the current space vector have been used as a new source of diagnostic data for stator and rotor induction motor faults [1,2]. These techniques depend upon specific harmonic components location in the motor current, which are usually different for different types of faults. Exploitation of instantaneous power factor is interesting because it varies according torque oscillation and hence the stator current [3]. Differential diagnosis is based on multivariable monitoring to assess induction machine rotor conditions [4]. The calculation of the negative impedance is used to the monitoring of the stator fault [5]. The major advantage of this technique is the non dependence on the slip. The negative sequence of the stator current represents a reliable index for the on line monitoring of stator unbalanced [6]. Exploitation of the line neutral voltage for the diagnosis of stator and rotor faults has been proposed [7]. Artificial Intelligence (AI) based on statistical machine learning approach [8], artificial neural networks [9], time–frequency for classification induction motor faults [10].

Recent advances and new techniques have been reported in the literature concerning calculation of faults in electrical machines these are; Multidimensional demodulation techniques for diagnosis of induction motors faults [11], polynomial-phase transform of the current for diagnosis of three-phase electrical machines [12], symmetrical components and current Concordia of an induction motor by feature pattern extraction method and radar analysis [13], Monte Carlo approach for calculating the thermal lifetime of

* Corresponding author.
  E-mail address: lebaroud@yahoo.fr (A. Lebaroud).

transformer insulation [14], intelligent approach by an artificial immune system for the detection of induction machines faults [15], independent component analysis for fault detection and diagnosis of turbine [16], signature analysis for fault diagnosis of mixed eccentricity [17].

FFT algorithm is one of the most popular signal-processing algorithms in motor-fault-detection applications. However, in real-time applications, the $(N/2) * \log(N)$ complexity of FFT-radix 2 brings an overwhelming burden to the DSP where significant amounts of data need to be processed in order to produce sufficiently high resolution [18]. The problem in the spectral approach is that we intend to use systematically the Fourier transforms and its different variants particularly the fast Fourier transform (FFT), for signals of machine faults whose frequencies are known before hand. It means that we calculate the remain of frequencies without need them and therefore the calculations are cumbersome and unnecessary.

In this paper we will investigate the applications of Discrete Fourier Transforms on the complex vector of three-phase stator currents; this will allow making the choice on the most appropriate alternatives to the calculation of the faults components at lower computational cost. We will begin this work by the presentation of a three phase unbalanced system and harmonic pollution. The Fourier transformed applied to three-phase system will allow understanding and calculating the unbalanced current caused by the negative system. Recursive Fourier Transform (RFT) will highlight the sidebands of broken bar fault without the presence of the fundamental, which at low spectral resolution or at low load inhibit these sidebands. This technique is also used in real time. The technique of phase spectrum allows us to better characterize the fault rupture bar. In order to make the technique less sensitive to harmonic pollution we proposed the technique of phase of the analytical signal. The spectrum of the instantaneous power facilitates the detection at low frequencies of few Hertz.

2. Spectral analysis of stator current vector

The spectral analysis of stator current is a powerful analytical tool that can highlight the presence of characteristic frequencies, including those related to faults.

2.1. Unbalanced and polluted three-phase system

A balanced system of three-phase current represents only a system of positive sequence; in contrast, an unbalanced system of three-phase current can be represented by the combination of positive sequence system, negative sequence system and homopolar system. In a system where the neutral is not connected, the current in the phase "m" is written in general form:

$$i_m(t) = \sum_{k \in \{-1,1\}} \sum_{h=0}^{n} I_{6h+k} \sqrt{2} \cos\left((6h+k)\omega_s t + \varphi_{h,k} - k(m-1)\frac{2\pi}{3}\right)$$

(1)

where I_{6h+k} is the fundamental RMS value for ($h = 0$), remained harmonics ($h \neq 0$), positive sequence ($h = 1$) or negative sequence ($h = -1$).

The development of eq. (1) yielded a vector of stator currents following:

$$\bar{i}_s = I_1 \sqrt{2} e^{j(\omega_s t - \varphi_1)} + \sum_{h=1}^{n} I_{6h+1} \sqrt{2} e^{j((6h+1)\omega_s t - \varphi_{6h+1})}$$

$$+ I_{-1} \sqrt{2} e^{-j(\omega_s t - \varphi_{-1})} + \sum_{h=1}^{n} I_{6h-1} \sqrt{2} e^{-j((6h-1)\omega_s t - \varphi_{6h-1})}$$

(2)

From Eq. (2) the complex magnitudes of different components are defined by:

$$\bar{I}_{6h+k} = I_{6h+k} e^{kj(6h+k) - \varphi(6h+k)}$$

(3)

Stator current vector becomes:

$$\bar{i}_s = \sum_{h=0}^{n1} \bar{I}_{6h+1} e^{j(6h+1)\omega_s t} + \sum_{h=0}^{n1} \bar{I}_{6h-1} e^{-j(6h-1)\omega_s t}$$

(4)

Equation of the stator current vector (4) is composed of two systems, one of positive sequence:

$$\bar{i}_p = \sum_{h=0}^{n1} \bar{I}_{6h+1} e^{j(6h+1)\omega_s t}$$

(5)

And the other negative sequence:

$$\bar{i}_n = \sum_{h=0}^{n1} \bar{I}_{6h-1} e^{-j(6h-1)\omega_s t}$$

(6)

$$\bar{i}_s = \bar{i}_p + \bar{i}_n$$

(7)

In the complex plane, the stator current vector of positive sequence has a circular shape. During the time of unbalanced fault, a negative sequence current appears and transforms the circular shape of the current vector to an elliptical shape. The spectrum of the stator current phase does not permit having the negative component of the current. On the other hand, the spectral analysis of the stator current space vector allows the separation of two of sequences: one positive defined in $[0 \quad f_{max}]$ and the other negative defined in the $[-f_{max} \quad 0]$. Fourier analysis is one of nonparametric methods of spectral estimation. Its application to analyze the stator current vector will provide further information on its spectral content.

2.2. Discrete Fourier Transform of stator current vector

The discretization of the stator current vector (4) gives the following equation:

$$[\bar{i}_s(n)] = \left[\bar{I}_1 e^{\frac{2\pi n f_s}{N}} + \sum_{h=1}^{n} \bar{I}_{6h+1} e^{\frac{2\pi n(6h+1)f_s}{N}} + \bar{I}_{-1} e^{\frac{2\pi n f_s}{N}} + \sum_{h=1}^{n} \bar{I}_{6h-1} e^{\frac{2\pi n(6h-1)f_s}{N}} \right]$$

(8)

The Discrete Fourier Transform of this vector is evaluated within the meaning of [19] to determine the harmonics of a Fourier series:

$$\bar{I}(f_k) = \frac{1}{N} \sum_{N=0}^{N-1} \bar{i}_s[n] \cdot e^{-j\frac{2\pi kn}{N}}$$

(9)

With:

$$W^{k \cdot n} = e^{-j\frac{2\pi kn}{N}}$$

(10)

We obtain the following notation with

$$[\bar{I}](f_k) = \frac{1}{N} [W^{kn}][\bar{i}_s(n)]$$

(11)

The DFT is characterized by:
An acquisition time: $T = \frac{N}{f_e}$.
The maximum frequency of the signal: $f_{max} = \Delta f \cdot N/2$ and the Nyquist frequency: $f_e = 2 \cdot f_{max}$.
The multiplication of the rotation matrix $[W^{nk}]$ by the current vector allows separation of the positive and negative sequences of the current vector:

$$[\bar{I}(f_k)]^t = [\ldots, \bar{I}_1, \ldots, \bar{I}_7, \ldots, \bar{I}_{6h+1}, \ldots, \bar{I}_{6h-1}, \ldots, \bar{I}_5, \ldots, \bar{I}_{-1}, \ldots]$$

(12)

In Eq. (12), $[\bar{I}(f_k)]$ is a vector representing the *k*th harmonics of the stator current vector i_s, in the frequency domain, while the vector $[\bar{I}_s(n)]$, in (8) represents the *N*th samples of the stator current vector in the time domain.

The calculation by the DFT of the *k*th frequency components from the *N*th samples of the current vector requires N^2 complex multiplications for $k = N$, which represents a very important volume calculation. Many elements of the rotation matrix are equal. The fast Fourier transform (FFT) exploits this advantage in order to reduce the volume of calculation. The algorithm of Cooley–Tukey is the most used among several other algorithms of the FFT. A reduction of N^2 complex operations to $(N/2)\log_2(N)$ arithmetic operations. For example, with a number of samples $N = 1000$, the DFT requires one million complex operations, while the FFT requires only 4982 operations, a reduction of about 200 times. Therefore, the FFT algorithm is widely used for the frequencies treatment of temporal signals. The rotation matrix $[W^{kn}]$ in Eq. (13), does not keep the same sign: of the line $k = 1,...,N/2$, the matrix is defined in a positive sequence, of the line $k = N/2,......,N$ the matrix is defined in a negative sequence, This allows to rewrite the matrix as follows:

$$[W^{kn}] = \begin{bmatrix} W_d^{nk} \\ W_i^{nk} \end{bmatrix} \tag{13}$$

The multiplication the rotation matrix $[W^{nk}]$ by the current vector is used to separate both the positive and negative sequences contained in the current vector as:

$$\begin{bmatrix} \bar{I}_{f1} \\ \vdots \\ \bar{I}_{f_s} \\ \vdots \\ \bar{I}_{(6\eta+1)f} \\ \vdots \\ \bar{I}_{(6\eta-1)f} \\ \vdots \\ \bar{I}_{-f_s} \\ \vdots \end{bmatrix} = \frac{1}{N} \begin{bmatrix} \sum_{h=0}^{n1} \bar{I}_{(6h+1)} W^{(1-(6h+1)f_s)n} + \sum_{h=0}^{n1} \bar{I}_{(6h-1)} W^{(1+(6h-1)f_s)n} \\ \vdots \\ \bar{I}_1 + \sum_{h=1}^{n1} W^{6hf_s n} + \bar{I}_1 W^{2f_s n} + \sum_{h=1}^{n1} \bar{I}_{(6h-1)} W^{6hf_s n} \\ \vdots \\ \bar{I}_{(6\eta+1)} + \sum_{h=0,h\neq\eta}^{n1} I_{(6h+1)} W^{6(\eta-h)f_s n} + \sum_{h=0}^{n1} I_{(6h-1)} W^{6(\eta+h)f_s n} \\ \vdots \\ \sum_{h=0}^{n1} I_{(6h+1)} W^{6(\eta-h)-2)f_s n} + \bar{I}_{(6\eta-1)} + um_{h=0,h\neq\eta}^{n1} I_{(6h-1)} W^{(6(\eta+h)-2)f_s n} \\ \vdots \\ \bar{I}_1 W^{-2f_s n} + \sum_{h=1}^{n1} \bar{I}_{(6h+1)} W^{-(6h+2)f_s n} + \bar{I}_{-1} + \sum_{h=1}^{n1} \bar{I}_{(6h-1)} W^{(6h-2)f_s n} \\ \vdots \end{bmatrix} \tag{14}$$

$$[\bar{I}(f_k)]^t = [\ldots, \bar{I}_1, \ldots, \bar{I}_7, \ldots, \bar{I}_{6h+1}, \ldots, \bar{I}_{6h-1}, \ldots, \bar{I}_5, \ldots, \bar{I}_{-1}, \ldots] \tag{15}$$

The spectrum given by (15) shows that the calculation of the negative sequence current $\bar{I}_{-1}$ inevitably involves the calculation of the positive components sequences for $k = 1, \ldots, N/2$, $[I(f_{6h+1})]$, which is a long and unnecessary computation. To avoid starting with the direct components, it is proposed to calculate the FFT of the current space vector of negative sequences.

$$\bar{i}_n = \frac{2}{3}\left(i_a(t) + a^2 \cdot i_b(t) + a \cdot i_c(t)\right) \tag{16}$$

The discretization of the current vector of negative sequence is presented as follows:

$$[i_n(n)] = \left[\bar{I}_{-1} W^{-nf_s} + \sum_{h=1}^{n1} \bar{I}_{6h-1} W^{-n(6h-1)f_s} + \bar{I}_1 W^{nf} + \sum_{h=1}^{n1} \bar{I}_{6h+1} W^{n(6h+1)f_s}\right] \tag{17}$$

It is possible to calculate the negative sequence component (I_{-1}) directly from the current vector. While in the previous case, the entire spectrum of the DFT contains frequencies less interesting, especially the low frequencies below 50 Hz, which require an acquisition time of 0.98 s for a spectral resolution of 1 Hz (l equivalent of 49 fundamental periods). It suffices one period to calculate the negative sequence component. However we can, in this case, reduce the duration of measurement to one period. Thus the number of samples becomes:

$$N = \frac{f_e}{f_s} \tag{18}$$

f_e is the sampling frequency and f_s is the stator frequency.

Discrete Fourier Transform performed by the FFT algorithm requires, nonetheless, a significant number of complex operations of multiplications and additions. Thus the systematic calculation of all frequencies in the signal represents a significant volume of calculations. To relax this technique, we must extract only the negative sequence of imbalance.

2.3. Detection by Recursive Fourier Transform (RFT)

Many faults (problems with motor coupling load, broken rotor bars) may cause fluctuations of torque and speed. They are manifested by the modulation of the amplitude and the frequency of stator current. This modulation is characterized by harmonics at low frequencies around of fundamental frequency. Given the magnitude of the amplitude of the fundamental against other current components, the elimination of this component in real time allows [20]:

– Improving the signal acquisition.
– Enhanced detection of components near the fundamental.

Recursive Fourier Transform (FFT) allows a real-time detection without the presence of the fundamental.

The recursive average of the Fourier transform is an iterative technique giving the amplitude and phase of any harmonic, provided that its frequency is known. The technique of Recursive Fourier Transforms allows an implementation in real time.

Assuming that the fundamental harmonic is sought, the fundamental is given by:

$$I_a = I_A \cos(\omega_0 m\Delta t) + I_B \sin(\omega_0 m\Delta t) \tag{19}$$

The magnitudes I_A and I_B are calculated recursively by [20]:

$$I_A(m) = I_A(m-1) + \frac{2}{N}\left[I_a(m) - I_a(m-N_p)\right]\cos\left(\frac{2\pi m}{N_p}\right) \tag{20}$$

$$I_B(m) = I_B(m-1) + \frac{2}{N}\left[I_a(m) - I_a(m-N_p)\right]\cos\left(\frac{2\pi m}{N_p}\right) \tag{21}$$

N is the samples number.

The amplitude and phase of the fundamental is given by:

$$I_a = \sqrt{I_A^2 + I_B^2} \tag{22}$$

$$\varphi_0 = \arctan\frac{I_A}{I_B} \tag{23}$$

To remove the fundamental component, the frequency band width to eliminate must be determined as follows:

$$\Delta f = \pm\frac{f_e}{N} \tag{24}$$

f_s is the sampling frequency and N is the samples number.

3. Techniques of the stator current phase

3.1. Spectrum phase

The spectrum phase is usually used in image processing where the phase of the analyzed signal contains more relevant information than the magnitude. The stator current spectrum phase provide signs of detection very interesting because these signs are very sensitive to variations caused by the break of bars and allows incipient detection of rotor fault.

The calculation of the phase is limited to four quadrants of the unit circle where the variations are between $-\pi$ and $+\pi$ result of the Fourier transform (9) written as:

$$F(k) = \mathscr{R}(F(k)) + j\mathscr{I}(F(k)) = F_{Re}(k) + jF_{Im}(k)$$

The phase of the Fourier transform $F(k)$ is given by:

$$\varphi(TF(k)) = \arctan\left(\frac{F_{Im}(k)}{F_{Re}(k)}\right) \tag{25}$$

3.2. Phase of analytical signal

The sensibility of the spectrum phase is also affected by harmonic currents. To solve this problem, we use the analytical signal phase, which means, applying Hilbert transform to the magnitude of the stator current spectrum.

The phase of analytical signal is based on calculating the phase of analytic signal obtained by a Hilbert transform of modulus of spectrum of current of induction machine [21]. This means that works directly on the modulus of the Fourier transform. The Hilbert transform of a signal returns a representation of this signal in the same field. In other words the Hilbert transform of modulus of the Fourier transform of stator current will result in a signal expressed in the frequency domain.

The Hilbert transform in the time domain corresponds to a phase shift of value $\pi/2$ of all the terms of the Fourier transform. It allows to change the cosines terms in sinus terms and sinus terms in cosines negative terms.

The Hilbert transform of a signal $y(t)$ can be written as

$$y(t) \xrightarrow{TH} \tilde{y}(t) = \tilde{y}_{Re}(t) + j\tilde{y}_{Im}(t)$$

where $\tilde{y}_{Im}(t)$ is the Hilbert transform of signal $\tilde{y}_{Re}(t)$. The signal, $\tilde{y}(t)$ is called the analytic signal.

Amplitude modulation $A(t)$ of time signal $y(t)$ is calculated using the following equation:

$$A(t) = \sqrt{\tilde{y}_{Re}(t)^2 + \tilde{y}_{Im}(t)^2} \tag{26}$$

Phase modulation φ is calculated by the following equation:

$$\varphi(t) = \arctan\frac{\tilde{y}_{Im}(t)}{\tilde{y}_{Re}(t)} \tag{27}$$

Fault diagnosis by the Hilbert transform is based on the calculate of the phase of analytical signal obtained by a Hilbert transform of module of current spectrum, its phase is irrelevant in this case.

4. Frequency analysis of the instantaneous power

The instantaneous power of a phase is the product of the supply voltage at the stator current. Indeed, the spectrum of the instantaneous power contains additional components located near the frequency of the fault as shown by the following equation [21].

$$p_s(t) = p_{s0}(t) + \frac{mV_{LL}I_L}{2}\left[\cos\left((2\omega_s - \omega_f)t - \varphi - \frac{\pi}{6}\right) \right.$$
$$\left. + \cos\left((2\omega_s + \omega_f)t - \varphi - \frac{\pi}{6}\right) + 2\cos\left(\varphi + \frac{\pi}{6}\right)\cos(\omega_f t)\right] \tag{28}$$

where

$$p_{s0}(t) = V_{LL}I_{LL}\left[\cos\left(2\omega_s t - \varphi - \frac{\pi}{6}\right) + \cos\left(\varphi + \frac{\pi}{6}\right)\right] \tag{29}$$

In this expression, $p_s(t)$ represents the instantaneous power of a phase stator m, the modulation index V_{LL}, the RMS value of the voltage between phase, I_L line current and ω_f oscillation pulse (pulsation of fault) in radians.

The terms ω_s and φ represent respectively the pulse of supply currents in radians and the dephasing angle between the absorbed current by the motor and the tension.

5. Experiment results

The experimental bench consists of a three-phase asynchronous motor squirrel cage Leroy Somer LS 132S, IP 55, Class F, T° C standard = 40 °C. The motor is loaded by a powder brake. Its maximum torque (100 Nm) is reached at rated speed. This brake is sized to dissipate a maximum power of 5 kW. Fig. 1 shows the motor bench.

The Leroy Somer motor parameters used in experiments are given below:

Rated power	5.5 kW
Number of poles	2
Rated voltage	230/400 Volts
Rated current	11.4 Amp
Rated frequency	50 Hz
Power factor	0.84
Rated speed 1	440 r/min
Number of stator slots	48
Number of rotor bars	28

For the rotor fault, the bar has been broken by drilling bar of cage squirrel (Fig. 2). The 5% of power imbalance for simulating the fault of stator unbalanced, is obtained with a variable auto-transformers placed on a phase of the network (Fig. 1). The acquisition of current signals was carried out on a test bench, The sampling rate is 10 kHz. The number of samples per signal rises at $N = 10,000$ samples.

A short circuit in the stator windings generates an unbalance of the currents that provides a negative spectral component $-f_s$ (Figs. 3 and 4). The amplitude of this component increases with the severity of the fault. The presence of broken bars fault at same time
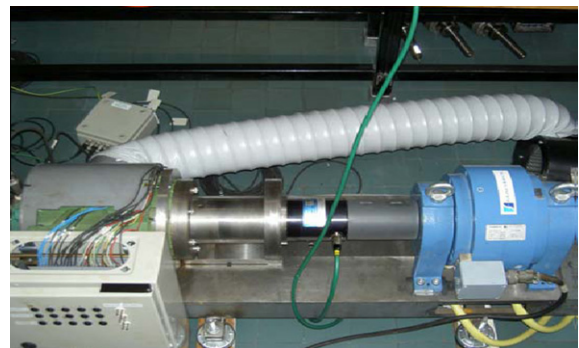

Fig. 1. Test bench of induction motor.
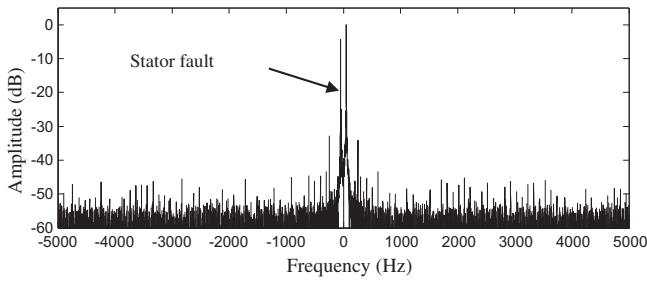
Fig. 2. Broken rotor bars.
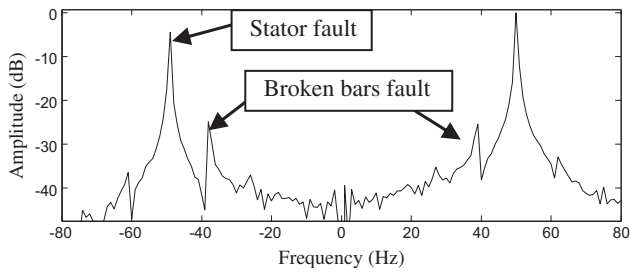

Fig. 5. Spectrum of stator current of rotor fault without fundamental (solid line) with the fundamental (dashed line).

Fig. 3. Spectrum of stator current vector.

Fig. 6. Phase of current spectrum (without supply by inverter), faulty (top), healthy (bottom).

Fig. 4. Zoom of spectrum of stator current vector.

Fig. 7. Phase of analytical signal of induction motor current (with supply by inverter) faulty (top), healthy (bottom).

that a stator fault causes the appearance of two lateral components, one the frequency $(1 - 2s)f_s$ at left of fundamental f_s and the other the frequency $-(1 - 2s)f_s$ to the right $-f_s$ (negative sequence component). The calculation of two fault components $(1 - 2s)f_s$ and $-f_s$ which causes problem, because we usually use the FFT to compute of frequencies known a priori. Knowing that the FFT does not calculate a single frequency but all the frequencies contained in the signal and sampling frequency.

The fast Fourier transform (FFT) does not allow a good legibility of harmonic frequencies of defaults $-f_s$ and $(1 - 2s)f$ because of number very high of frequencies. The search for these two frequencies of faults requires the calculation of $f_e/2 - 2$ unnecessary frequency.

For example with the sampling frequency $f_e = 10$ kHz we get $10,000/2 - 2 = 4998$ calculated frequencies uselessly and uninteresting. Even the zoom effect of the figure does not solve this problem because the calculations are already done.

The harmonic of rotor fault at the frequency $(1 - 2s)f$ is always close to fundamental, in order that it does not inhibit the emergence of fault harmonic of small magnitude, especially for the low spectral resolution or at low load, when the fundamental is removed, in this case the concerned harmonic becomes clear. The
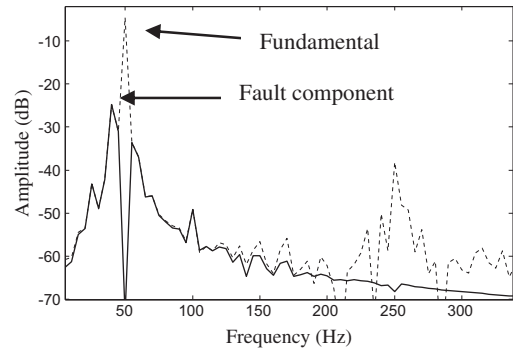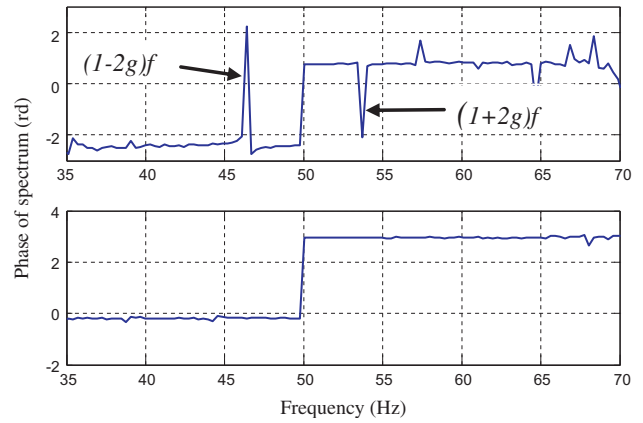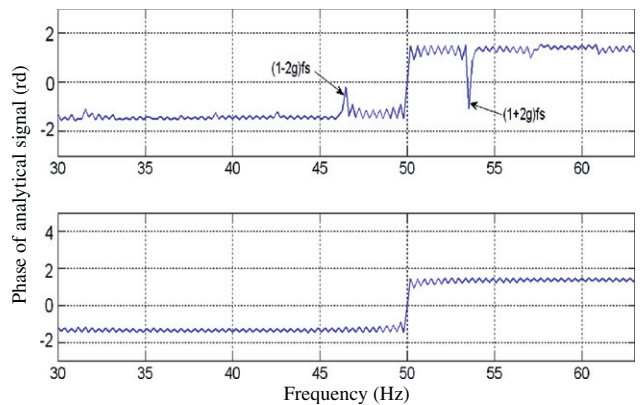
advantage of the RTF is its realization in real time. Fig. 5 shows a fault of broken bars. The sampling frequency of the signal acquisition is 10 kHz, the number of samples $N = 2000$, the width of the frequency: $2\Delta f = 10$ Hz. With the elimination of fundamental and the use of low pass filtering 160 Hz, the spectra of fault located in the frequency band [0 150] Hz are visible and well defined.

Unlike spectral analysis, the frequency resolution does not affect the abrupt change that occurs on the phase at 50 Hz, which facilitates the detection of the phase jump at frequency $(1 - 2g)f_s$ (Fig. 6). Disturbances generated by the inverters in the phase of
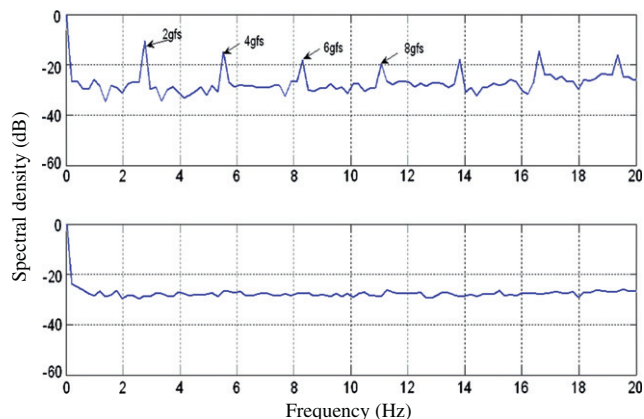
Fig. 8. Spectrum of the instantaneous power, faulty (top), healthy (bottom).

the stator current spectrum can affect fault detection. The technique of the analysis phase can overcome this drawback. Fig. 7 represent the phase of analytical signal of induction motor current with a healthy rotor and a rotor with a broken bar. This figure illustrates the presence of "phase jumps" to frequencies of faults $(1 \pm 2ks)fs$. It should also be noted that the appearance of rotor fault contributes to increase the amplitude of the jumps present in the phase $\varphi_{TH}(f)$.

Fig. 8 reveals the presence of low frequency components in the case of broken rotor bars. These components of fault appear more clearly than those of the stator current spectrum, this facilitates detection. Therefore they allow a significant improvement in fault diagnosis.

6. Conclusion

The RFT technique improves the signal acquisition and allows enhanced detection of the fault component near the fundamental. RFT allows a real-time detection without the presence of fundamental. In instantaneous power the faults components appear more clearly than those of stator current spectrum, thus easier to detect. In the phase of current Spectrum, the abrupt change that occurs on the phase at 50 Hz, facilitates the detection of the phase jump.

Phase of analytical signal improves the detection same with the presence of disturbances generated by the inverters in the phase of the stator current.

Acknowledgements

References

[1] Cruz SM, Cardoso AJM. Rotor cage fault diagnosis in three-phase induction motors by extended park's vector approach. Electr Mach Power Syst 2000;28(4):289–99.
[2] Perovic DK, Arkan M, Unsworth P. Induction motor fault detection by space vector angular fluctuation, vol. 1. Rome Italy: IEEE IAS; 2000. p. 388–94.
[3] Ibrahim Ali, El Badaoui Mohamed, Guillet François, Bonnardot Frédéric. A new bearing fault detection method in induction machines based on instantaneous power factor. IEEE Trans Ind Electron 2008;55(12):4252–9.
[4] Concari C, Franceschini G, Tassoni C. Differential diagnosis based on multivariable monitoring to assess induction machine rotor conditions. IEEE Trans Ind Electron 2008;55(12):4156–66.
[5] Henao H, Capolino GA, Assaf T, Cabanas MF, Melero MG, Orcajo GA, et al. A new mathematical procedure for the computation of the equivalent inverse sequence impedance in working induction motors. In: Industry applications conference, vol. 1, Rome, Italy; 2000. p. 336–43.
[6] Abdesselam Lebaroud, Guy Clerc, Abdelmalek Khezzar, Ammar Bentounsi. Comparison of the induction motors stator fault monitoring methods based on current negative symmetrical component. EPE J 2007;17(1).
[7] Khezzar A, El Kamel Oumaamar M, Hadjami M, Boucherma M, Razik H. Induction motor diagnosis using line neutral voltage signatures. IEEE Trans Ind Electron 2009;56(11):4581–91.
[8] Yeh CC, Povinelli RJ, Mirafzal B, Demerdash NAO. Diagnosis of stator winding inter-turn shorts in induction motors fed by PWM-Inverter drive systems using a time-series data mining technique. In: Proceedings of IEEE international conference on power system technology, Singapore; 2004 November 21–24. p: 891–6.
[9] Filippetti F, Franceschini G, Tassoni C, Vas P. AI techniques in induction machines diagnosis including the speed ripple effect. IEEE Trans Ind Appl 1998;34:98–108.
[10] Lebaroud, Clerc G. Classification of induction machine faults by optimal time–frequency representations. IEEE Trans Ind Electron 2008;55(12):4290–8.
[11] Choqueuse V, Benbouzid MEH, Amirat Y, Turri S. Diagnosis of three-phase electrical machines using multidimensional demodulation techniques. IEEE Trans Ind Electron 2012;59(4):2014–23.
[12] Pineda-Sanchez M, Riera-Guasp M, Roger-Folch J, Antonino-Daviu JA, Perez-Cruz J, Puche-Panadero R. Diagnosis of induction motor faults in time-varying conditions using the polynomial-phase transform of the current. IEEE Trans Ind Electron 2011;58(4):1428–39.
[13] Surajit Chattopadhyay, Subrata Karmakar, Madhuchhanda Mitra, Samarjit Sengupta. Symmetrical components and current Concordia based assessment of single phasing of an induction motor by feature pattern extraction method and radar analysis. Int J Electr Power Energy Syst 2012;37(1):43–9.
[14] Abu-Elanien Ahmed EB, Salama MMA. A Monte Carlo approach for calculating the thermal lifetime of transformer insulation. Int J Electr Power Energy Syst 2012;43(1):481–7.
[15] Chilengue Z, Dente JA, Costa Branco PJ. An artificial immune system approach for fault detection in the stator and rotor circuits of induction machines. Electr Power Syst Res 2011;81(1):158–69.
[16] Ali Ajami, Mahdi Daneshvar. Data driven approach for fault detection and diagnosis of turbine in thermal power plant using Independent Component Analysis (ICA). Int J Electr Power Energy Syst 2012;43(1):728–35.
[17] Rajalakshmi Samaga BL, Vittal KP. Comprehensive study of mixed eccentricity fault diagnosis in induction motors using signature analysis. Int J Electr Power Energy Syst 2012;35(1):180–5.
[18] Seungdeog Choi, Bilal Akin, Rahimian Mina M, Toliyat Hamid A. Implementation of a fault-diagnosis algorithm for induction machines based on advanced digital-signal-processing techniques. IEEE Trans Ind Electron 2011;58(3).
[19] Andria G. Inverter drive signal processing via DFT and EKF. IEE proceedings Pt.B, vol. 137, no. 2; March, 1990.
[20] Costa FF et al. Improving the signal data acquisition in condition monitoring of electrical machines. IEEE Trans Instrum Measur 2004;53(4).
[21] Didier G. Modélisation et diagnostic de la machine asynchrone en présence de défaillances. PhD thesis, University of Henri Poincaré, Nancy-I, France; 2004.